# Optimising expansion deflection nozzles for vacuum thrust

**N. V. Taylor and C. M. Hempsell**
University of Bristol
Bristol, UK

## ABSTRACT

While expansion deflection (ED) nozzles have traditionally been considered primarily for use as altitude compensating devices to improve the performance of single stage to orbit vehicles, they also offer the potential for enhancing high altitude propulsion systems. If intended to only operate in near vacuum conditions, the complexity of analysis and inherent risks involved in the ED concept are greatly reduced. An integrated approach to the design and performance analysis of such nozzles is presented, comprising a mixture of computational fluid dynamics, the method of characteristics, and a semi-empirical model to allow full analysis of the closed wake flow-field of an ED nozzle. While it is demonstrated that the influence of the parameters used to define the throat region is critical to the successful application of the ED nozzle, it is also shown that with careful design the weight savings possible are significant. The analysis method itself is flexible and rapid, and lends itself well to incremental improvements in accuracy as the flow under consideration becomes better understood.

## NOMENCLATURE

| | |
|---|---|
| $A_E$ | nozzle exit c.s.a. |
| $A_t$ | throat area |
| $B$ | shock entropy function |
| $c_{pb}$ | base pressure coefficient |
| $c_{df}$ | forebody drag coefficient |
| $C_F$ | thrust coefficient |
| $C_F^\infty$ | vacuum thrust coefficient |
| $D$ | body diameter |
| $D_W$ | pintle drag |
| $F$ | largest c.s.a. of body |
| $F_H$ | base area |
| $G_t$ | minimum wall separation |
| $h$ | c.s.a. of pintle used in drag calcs. |
| $H$ | shear layer height |
| $H^*$ | height of shock formation |
| K1R | shear layer function |
| LRC | left running characteristic |
| M | Mach number |
| $M_E$ | nozzle exit Mach number (at wall) |
| $M_{par}$ | parallel flow Mach number |
| $P$ | pressure |
| $R_p^-$ | pre throat pintle wall radius |
| $R_p^+$ | post throat pintle wall radius |
| $R_t$ | throat radius |
| $R_w^-$ | pre throat outer wall radius |
| $R_w^+$ | post throat outer wall radius |
| $s$ | length of last LRC in nozzle |
| $U$ | velocity |
| $x_0$ | first outer contour point. |
| $y_d$ | minimum pintle radius |
| $\beta$ | shock angle |
| $\gamma$ | ratio of specific heats |
| $\delta$ | boundary-layer thickness |
| $\rho$ | density |
| $\sigma$ | co-ordinate conversion function |
| $\theta_t$ | nominal flow angle at throat |
| $\zeta_\tau$ | radial distance to throat centre |

**Paper No. 2882**. Manuscript received 27 February 2004, revised version received 26 August 2004, accepted 8 September 2004.

## 1.0 INTRODUCTION

The function of the nozzle on a rocket motor is to convert the randomly directed thermal energy released by the combustion process into a strongly directional, high speed flow. To date, all operational rocket systems have achieved this through nozzle contours based either upon conical or optimised bell shaped designs. However, greater performance is possible with the use of alternative advanced nozzle concepts, such as the expansion deflection (ED), or Plug (Figs 1 and 2). In both cases a central body is used to turn the accelerating flow through an angle before the throat (ED outwards, the Plug inwards). This results in a more rapid expansion in the supersonic region, and produces a shorter overall nozzle length. Within the atmosphere, a boundary is formed between the high speed core flow and the atmosphere (internally on an ED, externally with the Plug) which allows the atmospheric pressure to interact with the primary flow, and change the effective area ratio of the nozzle. This process is known as altitude compensation, and in an ideal case would result in approximately 15% greater total impulse delivered during a single-stage trans-atmospheric flight[1].

However, the design and analysis of these nozzles is complicated, for while the Reynolds number is high enough that the primary flow may be modelled as inviscid outside of thin attached boundary-layers, it contains sub-, tran-, and supersonic flows, and interacts with a flow region dominated by viscous effects (Figs 1-2). Initially, the Plug nozzle seemed most promising, and the bulk of advanced nozzle research concentrates on this type (e.g. Refs 2-6). However, it has several drawbacks (probably the most serious being the very narrow throat required, giving rise to heating and tolerance related issues[7]), and as yet no operational version of the type has successfully flown.

The ED concept provides an alternative design with a different set of difficulties. While the throat gap is larger, the principle argument against it has been a supposed inferior altitude compensation, due to the evacuation of the central viscous region by the surrounding supersonic gas[1-3]. While there is some experimental evidence that appears to contradict this (e.g. Ref. 2 and anecdotally in Refs 8-10 for more details see Ref. 11), what is certain is that this, combined with the complexity of its design, has resulted in little interest or development of the type since the late 1960s.

Recent work at the University of Bristol has demonstrated that the throat region configuration, wall contour design, and complexity of requisite analytical methods are greatly affected by the implications of achieving effective altitude compensation[11]. However, many potential propulsion systems operate only at high altitude, where altitude compensation is not relevant. If this is the case, the analysis of the ED nozzle not only becomes considerably simpler, but also shares greater commonality with methods used for conventional nozzles, particularly with respect to contour optimisation. The type also offers significant advantages compared to the Plug nozzle, having all the advantages of reduced length combined with a more conventional combustion chamber, and improved heat transfer characteristics in the throat region[12]. This paper explores the advantages of closed wake ED nozzles through the use of a combined computational fluid dynamics (CFD) and method of characteristics (MoC) mathematical model.

## 2.0 GENERAL BEHAVIOUR

At high altitude, the viscous region behind the base of the central pintle in an ED nozzle contracts in the downstream direction, and shrinks to approximately zero radius. Once this occurs, the viscous region is sealed from the atmosphere, and hence is invariant with further reductions in ambient pressure. In turn, no further alteration of the effectively inviscid flow (and hence wall pressures) is possible, and altitude compensation ceases. If the nozzle is only used at altitudes above the point at which the wake closes, after the transients of start-up no significant changes in the flow structure occur, and the complex behaviour associated with wake closure is avoided. Treating the wake as permanently closed allows the performance of the nozzle to be largely determined from an analysis of the transonic throat and inviscid supersonic flows alone. However, while a prediction of the detail of the flow within the wake is not required, a pressure will be

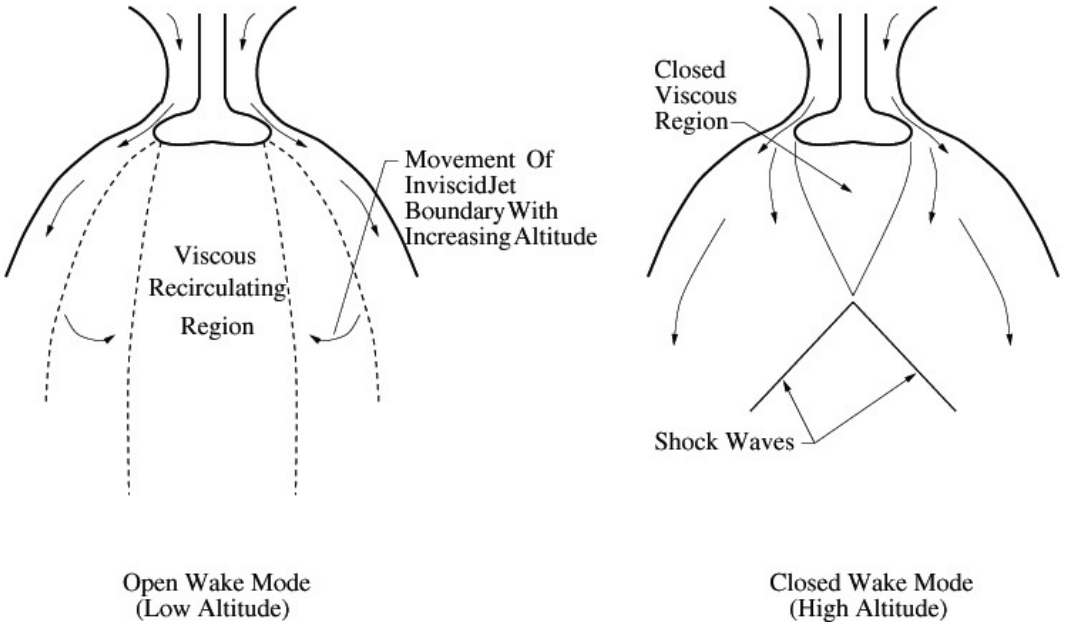


Figure 1. ED nozle general configuration.

https://doi.org/10.1017/S0001924000000348 Published online by Cambridge University Press

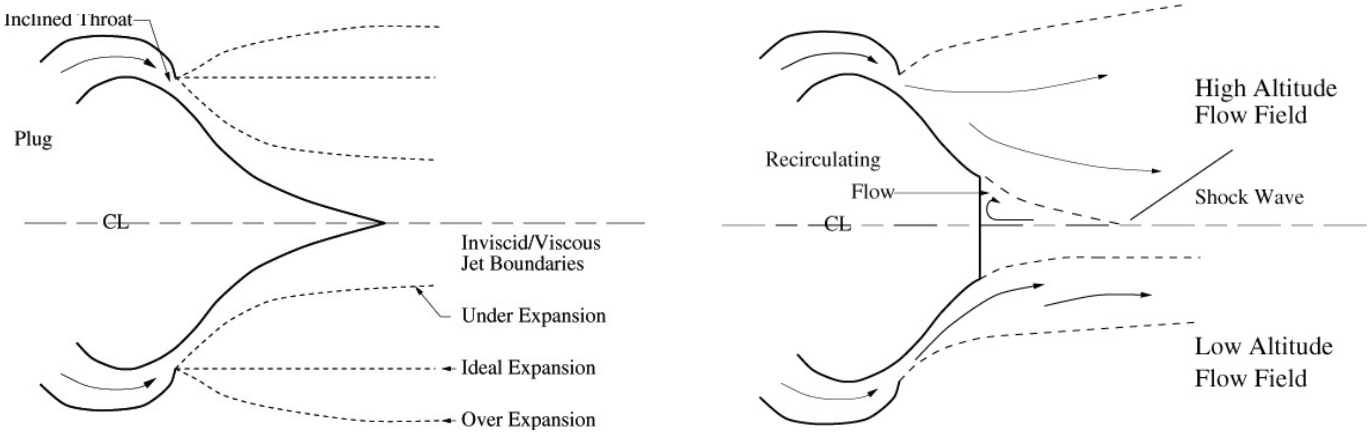


(a) Plug (b) Aerospike

Figure 2. Plug and aerospike nozzle general configuration.

exerted by the trapped gas on the base of the pintle, increasing thrust. Although likely to be relatively small, accurate calculation of vacuum performance entails the use of some method for estimating this base pressure.

One possible method would be an analysis of the entire flow using a CFD based method, and indeed this has been attempted for the analysis of altitude compensating Plug nozzle flows[4-6]. However, the requirement to model the viscous region and predict separation of the flow from the pintle would require the development and implementation of an advanced method, and hence be complex and time consuming. Alternatively, as the influence of the viscous region on the wall pressures has been removed by the closed wake assumption, independent solution methods for each of the three flow areas may be developed consecutively, from throat flow to base pressure, and the thrust developed at each stage combined to estimate the entire thrust of the nozzle. This is not only simpler and more rapid, but allows simple analytic optimisation methods to be employed in the contour design.

In the model developed at the University of Bristol, the throat region is analysed by a finite-volume central difference CFD scheme (based on the method of Jameson[13-15]), solving the Euler equations. Once an initial line is interpolated from the output of the CFD throat flow analysis, the method of characteristics (MoC) may be used to solve the remainder of the inviscid flow-field. This technique is fast and efficient, and more importantly allows optimisation of nozzle contours for minimum length via the well known method due to Rao[16], also adapted to ED nozzles by the same author[10]. This combined method has been demonstrated to be effective for solution of the inviscid flow-fields within conventional and unconventional nozzles[11,17,18].

This process, however, takes no account of the base pressure produced by the flow-field. It has therefore been extended to allow estimation of this contribution to thrust by incorporating a technique developed for analysis of blunt-based projectiles by Tanner[19,20]. This requires some adaption to allow its application to the problem of pintle base pressure prediction on ED nozzles, and hence a brief outline of the method, focusing on these alterations, is presented. The vacuum-optimised ED nozzle designs produced by this three component scheme are then discussed.

## 3.0 BASE PRESSURE PREDICTION

Previous efforts at calculating the closed wake base pressure of ED nozzles (most notably by Mueller *et al*[8,21]) have been based on variations of the mixing theories presented by Korst[22] and Chapman[23], combined with the MoC to allow calculation of the pressure distribution imposed by the inviscid flow-field. However, these attempts were not entirely successful, due primarily to two factors.

First, the difficulty of predicting the flow in the arbitrarily displaced and inclined axisymmetric throats associated with the nozzle type resulted in either linear Mach isobar approximations (poor even in many conventional nozzle cases, and more so for the ED), or empirical measurements being used. Such configurations present no difficulty to a CFD scheme however, which unlike the analytical methods available at the time of the aforementioned research is not based upon small perturbation assumptions. Second, the mixing theory itself requires a number of parameters to be empirically determined, and hence a more recent and simpler model is used here. It should be noted, however, that it too contains some empirical quantities, and was not originally designed for use in the prediction of ED flow-fields. It should therefore be viewed as an alternative (rather than superior) method at present, until sufficient experimental evidence becomes available for a quantitative comparison of the two.

### 3.1 The method of Tanner

By consideration and comparison of the inviscid and viscous flows past isolated bodies of revolution in a uniform supersonic flow field (Fig. 3), Tanner[19] has shown that:

$$\frac{c_{df}-c_{pb}}{-c_{pb}+8\frac{\delta_2}{D}-0\cdot008}\frac{F_H}{F}K_{1R}\left(\mathrm{M}_1\right)\frac{\gamma}{2}\mathrm{M}_1^2=\left(\frac{H^*}{H}\right)^2 B\left(\mathrm{M}_2,\beta\right) \quad \ldots (1)$$

where $F_H$ is the largest cross sectional area perpendicular to the flow, $F$ the base area of the object, $c_{df}$ the forebody drag coefficient, $c_{pb}$ the base pressure coefficient, $\delta$ the boundary-layer thickness at separation, $D$ the diameter of the object, subscripts 1 and 2 refer to freestream

https://doi.org/10.1017/S0001924000000348 Published online by Cambridge University Press

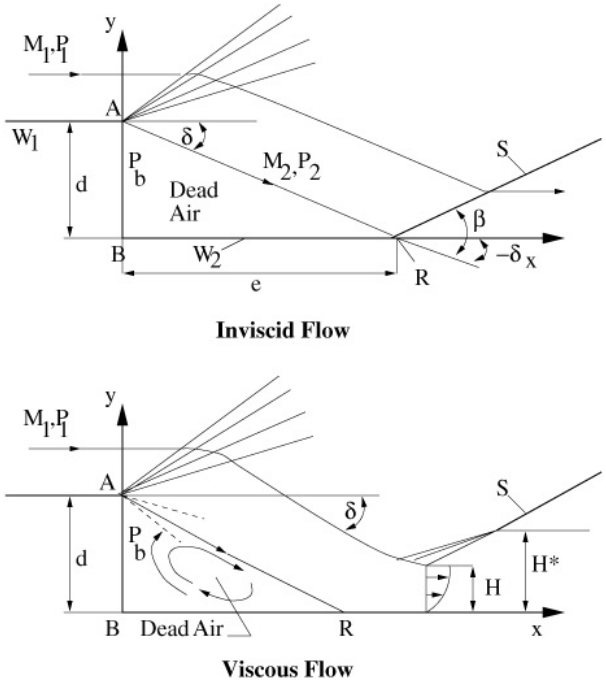


Figure 3. Tanner's flow models.

properties just before separation and recompression respectively, and the two functions $B(M_2,\beta)$ and $K_{1R}(M_1)$ are given by;

$$B\left(M_2,\beta\right)=\ln\left[\frac{\left(1+\frac{2\gamma}{\gamma+1}\left(M_2^2\mathrm{Sin}^2\beta-1\right)\right)^{\frac{1}{\gamma-1}}}{\left(\frac{(\gamma+1)M_2^2\mathrm{Sin}^2\beta}{(\gamma-1)M_2^2\mathrm{Sin}^2\beta+2}\right)^{\frac{\gamma}{\gamma-1}}}\right] \quad \ldots (2)$$

$$K_{1R}\left(M_1\right)=4\int_0^1\frac{\rho}{\rho_1}\frac{U}{U_1}\left(1-\frac{U}{U_1}\right)\frac{y}{H^2}\mathrm{d}y \quad \ldots (3)$$

$H$ being the height of the shear layer. This leaves one empirical quantity (representing the ratio of the minimum radius at which the shock wave exists to the shear layer thickness in the viscous flow regime):

$$\left(\frac{H^*}{H}\right)^2=2\left[1+\frac{1}{0\cdot00387M_2^{3\cdot2}}\right] \quad \ldots (4)$$

This method has been shown to provide good agreement with experimental results for a wide range of conditions[19-20,24].

### 3.2 Adaption to the ED nozzle

In the derivations of the methods based on mixing theories, and explicitly stated by Tanner, it is assumed that the problem under consideration is that of an isolated body immersed within a supersonic flow-field that is uniform at the upstream farfield boundary. The design of an ED nozzle violates these assumptions in three ways; the pintle is immersed within a non uniform flow-field (i.e. there is no unique $M_1$), the nozzle contour is in close proximity to the pintle, and there is no physical or representative farfield upstream supersonic boundary to allow calculation of the pressure coefficients. These considerations will obviously have an effect on the accuracy of the method applied to the ED problem, and are hence considered in order below.

The large pressure and velocity gradients in axial and radial directions due to wall curvatures in the throat region upstream of the point of separation will alter the shape of the Mach isobars at separation, perturbing them from the linear and parallel flow profile associated with the local flow before separation on a rearward step. An approximation to a uniform parallel upstream Mach number may be generated, however, by integrating an equivalent Mach number, $M_{par}$ along the last left running characteristic (LRC) in the nozzle flow computed during nozzle optimisation. This equivalent Mach number is found by expanding that actually calculated at each point by the MoC such that the flow becomes axial. The Mach number used within the solution equations is therefore;

$$M_1=\frac{1}{s}\int_{P\mathrm{int}le}^{Contour}M_{par}\mathrm{d}s \quad \ldots (5)$$

where $s$ is the length of the LRC from separation on the pintle to the tip of the contour. This simplification ignores all pressure gradient effects on the base flow region.

The proximity of the contour has no direct effect (although the Mach isobar distortion discussed above is in part due to this body), provided that the expansion waves created at the point of separation do not reflect from it and subsequently interfere with the base flow region. As the intersection of expansion waves with the contour may only occur if the flow is forced to separate before the intersection of the last LRC in the nozzle flow-field with the pintle wall by deliberately shortening the pintle, and that such a design would cause lowered wall pressures and hence reduced thrust, this is a reasonable assumption provided that the pintle is not translated from its design position (e.g. to allow throttling).

The onflow pressure and Mach number, $P_\infty$ and $M_\infty$, are approximated by averaging the pressure across the first row of cells from the converged CFD solution, which itself requires a length of parallel duct upstream of the throat to allow simple inflow boundary conditions. This represents a parallel undisturbed flow, although it should be noted that this is a subsonic boundary, and hence is not directly equivalent to the onflow conditions required for the standard Tanner model. The base pressure coefficient is then given by

$$c_{pb}=\frac{2}{\gamma M_\infty^2}\left[\frac{P_b}{P_\infty}-1\right] \quad \ldots (6)$$

For the forebody, the wall pressure drag $D_W$ may be found by integrating the pressure forces acting in the axial direction predicted at the wall by the CFD throat flow model up to the minimum geometric gap, and by the MoC solution from the geometric minima to the point of separation. The forebody drag coefficient is then calculated from

$$c_{df}=\frac{2}{\gamma h M_1^2}\left[\frac{D_W}{P_\infty}-1\right] \quad \ldots (7)$$

where $h$ is the base area of the pintle between the minimum and maximum radial extent of the pintle/flow boundary.

Experimental investigation of conventional throat geometries revealed that the boundary-layer thickness is extremely thin in the throat region[25], and there is no reason that this should be any different in the ED design. The pintle base is only a short distance downstream, in a favourable pressure gradient and against what is likely to be a highly cooled wall, and hence the boundary-layer at separation should also be extremely thin, and hence it is ignored in the current analysis. Even if of significant thickness (a few percent of pintle height), the error introduced would be in the region of one to two percent, based on a comparison of flow conditions with figures for boundary-layer effects presented in Ref. 19.

https://doi.org/10.1017/S0001924000000348 Published online by Cambridge University Press

**Table 1**
**Allowable $M_E$ Range for various nozzle configurations**

| Geometry Paramaters | | | | | | Allowable $M_E$ Range | | | | | |
|---|---|---|---|---|---|---|---|---|---|---|---|
| | | | | $R_{p,w}^-$ | | $R_w^+$ $R_p^+$+, in $G_t$ | | | | | |
| θ | $y_d$ | $\zeta_t$ | σ | | | | | | | | |
| deg | $G_t$ | $R_t$ | – | $G_t$ | $R_t$ | 5:5 | 5:2·5 | 5:0 | 2·5:5 | 2·5:2·5 | 2·5:0 |
| 60 | 1·5 | 1·76 | 0·28 | 5 | 1·39 | 3·4-4·9 | 2·8-5·1 | 2·7-5·2 | 3·6-4·7 | 2·8-4·8 | 2·6-5·0 |
| 60 | 8 | 2·47 | 0·20 | 5 | 1·01 | 3·3-5·2 | 2·8-5·4 | 2·6-5·5 | 3·5-5·0 | 2·8-5·1 | 2·6-5·4 |
| 90 | 1·5 | 2·26 | 0·22 | 5 | 1·10 | none | 4·2-4·5 | 3·7-4·7 | none | 4·2-4·4 | 3·7-4·6 |
| 90 | 8 | 2·90 | 0·17 | 5 | 0·86 | none | 4·2-4·8 | 3·7-5·0 | none | 4·3-4·7 | 3·7-5·0 |
| 60 | 4·5 | 2·46 | 0·20 | 10 | 2·01 | 3·4-5·2 | 2·7-5·4 | 2·5-5·6 | 3·5-5·1 | 2·8-5·2 | 2·5-5·4 |

### 3.3 Comparison with experiments

Once Equations (5-7) have been calculated, the values obtained are substituted into Equation (1), and following a simple iterative process, the base pressure for the pintle at vacuum conditions is obtained. This process is rapid, and does not require recalculation of the inviscid flow. This means that a single throat flow solution provided by CFD analysis may be fed to a combined MoC and base pressure code (the former incorporating an optimisation algorithm), and a series of nozzle lengths analysed far more rapidly than would be possible with either an iterative base pressure solver using a mixing theory or that of Tanner, or a complete CFD solution. However, this advantage is nullified if accuracy has been sacrificed. In order to determine the implications of the simplifying assumptions made above, it is necessary to compare predictions with experimental results.

While experimentally derived base pressures for flows past isolated bodies and simple rearward steps are fairly common in the literature, and used by both Tanner and the mixing theory schools for verifications of their respective methods, the specific problem of the pressure behind the pintle in an ED nozzle has received very little attention. In fact, the only published data for axisymmetric nozzles is given by Mueller[21].

The nozzles produced by Mueller make use of sharp edged pintles (i.e. $R_p^+ = 0$, see the following Section 4 for a full discussion of ED throat geometry). The contours are of ideal type, and hence the last characteristic in the flow is assumed to be describing parallel flow with a uniform Mach number which therefore corresponds directly to $M_1$. However, this is a calculated rather than measured variable, based on an assumption of uniform flow at the throat, and hence is unlikely to be completely accurate. Granting this assumption, the onflow Mach number is then a function primarily of throat angle. While values for the base area are not given, it has been shown that this has a relatively minor effect on the base pressure[11].

The data presented in Ref. 21 is in the form of a plot of the variation in $P_b/P_1$ with $M_1$. However, the experimental conditions are not fully disclosed, and the dimensions of the pintle are not given. Despite this, it is still possible to provide at least a qualitative comparison between the method described here and these experimental results, by calculating the base pressure behind various ED nozzles with pintles having sharp corners at the throat. The base area used for drag calculation (Equation (7)) was maintained at a constant value of $\pi R_t^2$, and the expansion fan was assumed to begin immediately after the throat. The pre throat curves on both outer and pintle contours were set to $2G_t$. Mesh size was 256 by 64 cells, and γ was set to 1·403 to simulate air (the working fluid used by Mueller in his experiments). The results of this analysis is shown in Fig. 4.

As may be seen, the general trends are similar, although the current model over predicts base pressure by approximately 20%. While this is a significant error, it should be remembered that the theoretical model is affected by the forebody shape of the pintle, not specified in the experimental results, that boundary-layers are ignored, and that the shape of the Mach contours in the experimental model is unknown. Finally, no assessment of possible experimental error is available.

The results presented in this figure demonstrate that the Tanner style analysis predicts that throat angle has no effect on the relationship of $M_1$ to $P_b/P_1$. It may also be seen that the current model more closely approximates the experimental results for small $M_1$. As large $M_1$ values will be associated with larger nozzles, and hence a greater dominance of the outer wall forces in the overall thrust prediction, the increased error in pressure prediction will have a much lesser impact in the accuracy of the final thrust prediction.

## 4.0 THROAT GEOMETRY DEFINITION AND EFFECTS

The purpose of the walls in the throat region of an ED nozzle is to redirect the incoming axial flow from the combustion chamber in such a manner that the nozzle throat is located at the required inclination and radial distance from the nozzle centreline. It is beneficial if this can be done in such a manner that the flow accel-

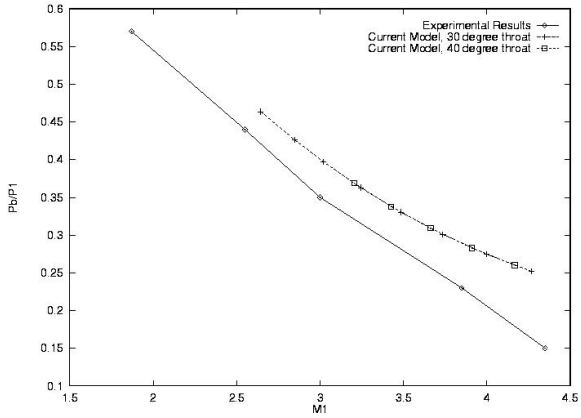


Figure 4. Base pressure comparison.

https://doi.org/10.1017/S0001924000000348 Published online by Cambridge University Press

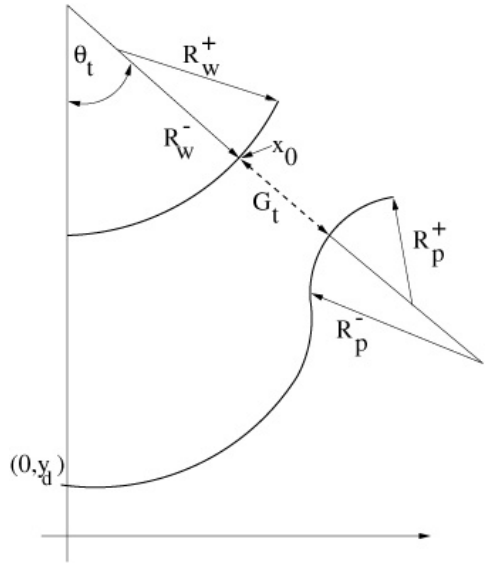


Figure 5. ED nozzle throat geometry.

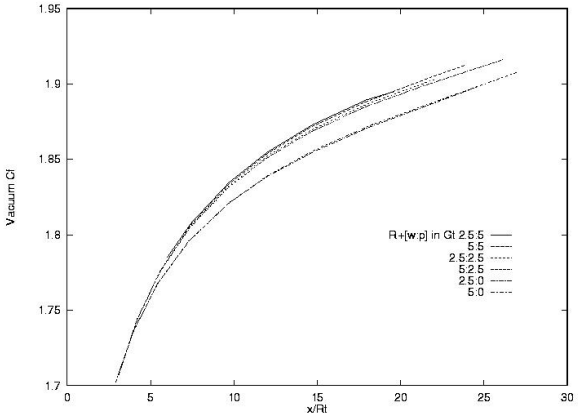


Figure 6. Effect of $R_w^+$+ and $R_p^-$+ on $C_F^\infty$, Axisymmetric ED Nozzles, $R_{=}^{-} = 5G_t$, $\theta_t = 60°$.

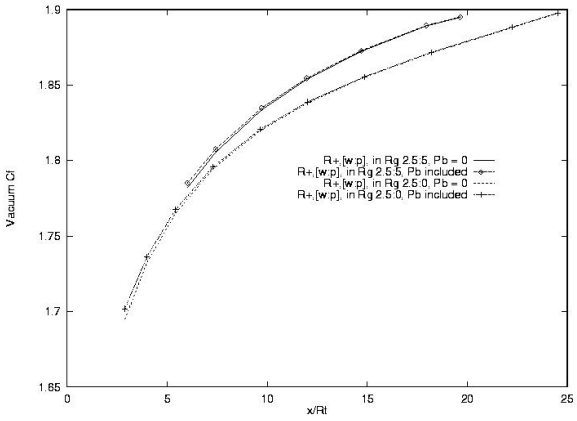


Figure 7. Contribution of $R_P$ to $C_F^\infty$, Axisymmetric ED Nozzles, $R_{=}^{-} = 5G_t$, $\theta_t = 60°$.

eration is smooth, but in the minimum axial distance to reduce overall nozzle length. Although the method used here (outlined graphically in Fig. 5, and discussed in more detail in Ref. 17) is not the only possible general formulation, it has been shown to reliably produce contours for a wide range of throat angles at various distances from the nozzle centreline.

While the specification of the throat region of a conventional nozzle is more or less completed by designating $R_w$, the wall radius of curvature, in order to uniquely define an ED configuration, $\theta_t$, the throat angle, $y_d$, the minimum pintle radius, and the pre and post throat radii of both the pintle and outer nozzle walls ($R_p^-$, $R_p^+$, $R_w^-$ and $R_w^+$ respectively) all need to be specified. All can have an impact on the nature of the flow field further downstream in the main part of the nozzle, potentially limiting the range of possible optimised contours to a narrow band of exit Mach numbers ($M_E$), and in turn a limited range of possible (optimised) nozzle lengths and area ratios. A brief assessment of the impact of these variables is therefore presented in Table 1 assuming a constant $\gamma = 1{\cdot}23$ (a more thorough discussion of this issue is contained in Refs 11 and 17).

In this table some dimensions are given in terms of $R_t$, the throat radius of a conventional nozzle having the same throat area as the specified ED. Generally, similar flow-fields are produced by similarity in the $G_t$ co-ordinate, whereas measurements in $R_t$ provide an indication of the size various dimensions would be on an ED nozzle replacing an existing conventional design. If $l$ is some length, then

$$l(R_t) = \sigma l(G_t) \qquad \ldots (8)$$

where

$$\sigma = \sqrt{\frac{\pi}{A_t}} \qquad \ldots (9)$$

and $A_t$ is the minimum cross sectional area between the ED nozzle walls when revolved through 360°. In physical terms, $\sigma$ represents the minimum separation of the nozzle walls in $R_t$ units, and hence allows a rough estimation of the likely magnitude of cooling difficulties (the heat flux for a constant chamber pressure being increased by a reduction of this minimum separation[12]).

This is only a small selection of input parameters and lengths that would give rise to physically possible throat configurations, but is sufficient to demonstrate the sensitivity of the optimisation process to the throat region (to give some idea of the restrictions implied by this table, note that for a one dimensional nozzle flow, $M_E$ of 3, 4 and 5 represent area ratios of 6·16, 23·2, and 83·9 respectively). That such limits on contour design for the ED nozzle have not been noted previously appears to be due to the fact that the problem is worsened by parameter selection that create throat flows outside the range of applicability of the simpler methods previously used, and hence this problem would not have occurred if, for instance, simple linear sonic lines were assumed (note that as a general rule, the range of area ratios possible is greater for large $R_w^+$ and $y_d$, which reduces the curvature of isobars at the throat). However, increasing $y_d$ or $R_w^+$ will inevitably reduce $\sigma$ (the throat is further from the axis, and hence for constant revolved area, the wall gap must reduce), increasing thermal management difficulties.

## 5.0 VACUUM PERFORMANCE

In the results presented, all the CFD grids used to generate the initial starting line for the MoC based method measured 256 by 64 cells, $\gamma$ was 1·23 to simulate LOx/LH products of combustion, and both $R_p^-$ and $R_w^-$ were set arbitrarily to $5G_t$ unless otherwise stated.

https://doi.org/10.1017/S0001924000000348 Published online by Cambridge University Press

**Table 2**
**Characteristics of axisymmetric nozzles, $C_F^\infty = 1{\cdot}830$**

| $\theta_t$ | $y_d$ | $R_w^-$ | $R_w^+$ | $R_p^-$ | $R_p^+$ | $x_E$, $R_t$ | $A_e/A_t$ |
|---|---|---|---|---|---|---|---|
| 0° | n/a | $3R_t$ | $R_t$ | n/a | n/a | 15·0 | 46·1 |
| 30° | $4{\cdot}5G_t$ | $5G_t$ | $5G_t$ | $5G_t$ | $2{\cdot}5G_t$ | 10·94 | 46·8 |
| 60° | $1{\cdot}5G_t$ | $5G_t$ | $5G_t$ | $5G_t$ | $2{\cdot}5G_t$ | 9·20 | 46·8 |
| 60° | $8G_t$ | $5G_t$ | $5G_t$ | $5G_t$ | $2{\cdot}5G_t$ | 7·82 | 45·4 |

ED nozzle lengths are defined as the distance between the intersection of the minimum wall separation and the outer wall contour (labelled $x_0$ on Fig. 5) and the exit plane. It is measured in $R_t$, the throat radius of an equivalent bell nozzle, which allows direct comparison of nozzle lengths.

The CFD model of the throat region allows the effect on vacuum thrust of arbitrary variations in the throat geometry parameters discussed in the previous section to be analysed. As an example, Fig. 6 demonstrates the influence of the wall radii of curvature on the outer and pintle walls after the throat. As may be seen, higher performance is achieved by increasing $R_p^+$, and to a lesser extent reducing $R_w^+$. These effects are more pronounced for small throat angles (60° being intermediate), and are in opposition to the trends identified previously as increasing the range of allowable $M_E$.

The $C_F^\infty$values shown in Fig. 6 include the contribution to thrust provided by the pressure exerted on the base of the pintle. As has been discussed, the accuracy of the predictive procedure used to generate this estimate is uncertain, as it is derived from a method for a slightly different flow problem and has yet to be fully experimentally verified in the specific case of ED nozzles. However, as Fig. 7 demonstrates, the contribution to total vacuum thrust is so small that even if the error produced is considerably greater than the 20% suggested by the results in Fig. 4 are occurring, the overall effect on nozzle thrust will be negligible. This also shows that the exclusion of base pressure prediction from the contour optimisation process, necessary to allow the calculus of variations method to be employed, is reasonable.

Figure 8 provides a performance analysis of length optimised contours produced by a selection of ED nozzle throat configurations. All the allowable nozzle lengths are shown for each, i.e. length optimised nozzles either shorter or longer than the extent displayed in Fig. 8 do not exist. The results presented in this figure clearly demonstrate the opposing effects of increasing $\theta_t$. While the vacuum thrust is increased for a given nozzle length, the possible range of lengths the nozzle may take is restricted. This may be partly offset by an increase in $y_d$, providing a greater allowable range and at the same time raising $C_F^\infty$, although this will inevitably lead to a reduced wall separation at the nozzle throat, with attendant heat transfer and manufacturing problems.

The same figure gives the relationship between nozzle length and vacuum thrust coefficient of a conventional bell nozzle, and this reveals that an ED nozzle which offers far greater performance may be chosen for any length. However, this increment in $C_F^\infty$ is in part explained by the decoupling of the expansion ratio from total nozzle length, and hence some care must be taken in interpreting this result. In essence, the greater thrust for a given length is produced due to a much larger expansion ratio, and hence the contour produces a considerably greater surface of revolution (and hence mass) when rotated about the nozzle centreline.

If instead of constant length, a pre-determined vacuum thrust is maintained, an ED contour considerably shorter than a bell may be designed. Table 2 presents lengths for an arbitrarily

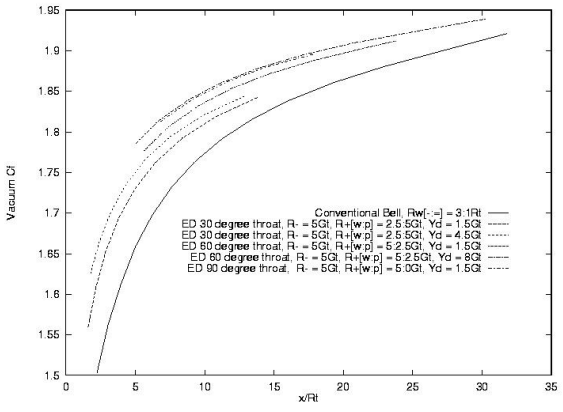


Figure 8. $C_F^\infty$ *vs* length, various nozzles.

selected $C_F^\infty$ of 1·830, while the contours (in the case of ED nozzles, outer walls only), are presented in Fig. 9. Reductions in length of up to 50% are possible from this relatively small selection of ED throat configurations. While the increased radial location of the nozzle contour downstream of the throat will mean that the direct saving on nozzle mass is considerably less than this, inter-staging mass and other nozzle length dependent factors should be reduced by much nearer the full 50%.

## 6.0 CONCLUSIONS

The results presented demonstrate that notable reductions in length are possible by applying the ED nozzle concept for the special case of nozzles restricted to high altitude applications. This in turn should result in mass savings when the knock on impact on the vehicle as a whole is considered.

A simple technique for predicting base pressures has been developed, and demonstrated to behave correctly in at least a qualitative fashion. While some work remains before it may be accepted to be accurately predicting the thrust produced from this region, analysis of the complete nozzle flows has shown that the influence of the accuracy of this method on the viability of

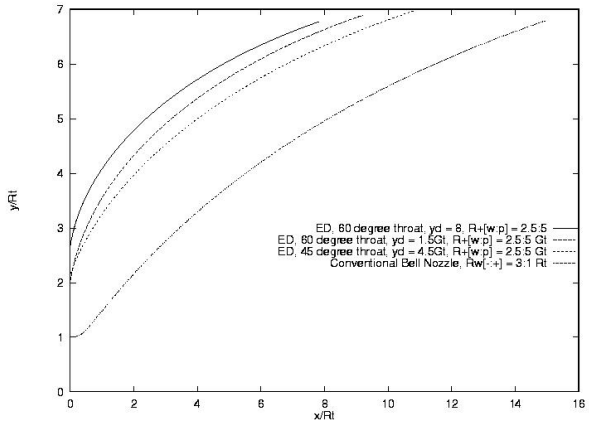


Figure 9. Contours for axisymmetric nozzles, $C_F^\infty = 1{\cdot}830$.

https://doi.org/10.1017/S0001924000000348 Published online by Cambridge University Press

the ED concept is minimal. Of far greater importance is the detail of the throat geometry which has a large effect on the permissible contours produced by the length optimising algorithm, and on the performance of the nozzle produced. The throat region of an ED nozzle will also be more difficult to cool than a conventional nozzle, with higher heat fluxes. Cooling requirements are not at present analysed in a quantitative manner, but will influence optimal throat configurations. This is because improved performance is always achieved by increasing the radial location of the throat, but this in turn reduces the throat gap, increasing heat fluxes.

The framework of the integrated method presented here allows for gradual improvement, primarily through inclusion of heat transfer properties through the nozzle and pintle walls, and boundary-layer behaviour both in the throat and contour regions. These two areas are now the largest obstacles remaining in the successful design, analysis, and application of the ED nozzle to high altitude environments.

## ACKNOWLEDGEMENTS

The authors would like to thank the EPSRC of the UK for funding the work presented in this paper.

## REFERENCES

1. HAGEMANN, G., IMMICH, H., NGUYEN, T.V. and DUMNOV, G.E. Advanced rocket nozzles. *J Propulion and Power*, September 1998, **14**, (5), pp 620-634.
2. MUELLER, T.J. and SULE, W.P. Annular truncated plug nozzle flowfield and base pressure characteristics. *J Spacecraft*, November 1973, **10**, (11), pp 689-695.
3. WASKO, R.A. Performance of annular plug and expansion-deflection nozzles including external flow effects at transonic mach numbers. Technical Report NASA-TN-D-4462, NASA, April 1968.
4. ROMMEL, T., HAGEMANN, G., SCHELY, C.A., KRULLE, G. and MANSKI, D. Plug nozzle flowfield analysis. *J Propulsion and Power*, September 1997, **13**, (5), pp 629-634.
5. F. NASUTI, and ONOFRI, M. Theoretical analysis and engineering modelling of flowfields in clustered module plug nozzles. *J Propulsion and Power*, July-August 1999, **17**, (4), pp 544-551.
6. NASUTI, F. and ONOFRI, M. Analysis of in flight behaviour of truncated plug nozzles. *J Propulsion and Power*, July-August 2001, **17**, (4), pp 809-817.
7. BEICHEL, R. Nozzle concepts for single stage shuttles. *Astronautics and Aeronautics*, June 1975, pp 16-27.
8. MUELLER, T.J., SULE, W.P. and HALL, C.R. Characteristics of separated flow regions within altitude compensating nozzles. Technical Report NASA-CR-116875, NASA, January 1971.
9. SCHORR, C. Constant chamber throttling of an expansoin deflection nozzle. *J Spacecraft*, July 1970, **7**, (7), pp 843-847.
10. RAO, G.V.R. Analysis of a new concept rocket nozzle. *J Liquid Rockets and Propellants*, 1960, 2:669:682.
11. TAYLOR, N.V. An Integrated Approach To Expansion Deflection Nozzle Analysis. PhD. Thesis, University of Bristol, 2002.
12. MAYER, E. Analysis of convective heat transfer in rocket nozzles. *ARS J*, July 1961, **31**, (7), pp 911-916.
13. JAMESON, A. Transonic aerofoil calculations using the euler equations. In *Roe*, P.L. (Ed), *Numerical Methods in Aeronautical Fluid Dynamics*, pp 289-309, 24/28 Oval Road, London, 1982. The Institute of Mathematics and its Applications, Academic Press.
14. SCHMIDT, W., JAMESON, A. and TURKEL, E. Numerical solutions of the euler equations by finite volume methods using runge-kutta time stepping schemes. AIAA-Paper No 81-1259, 1981.
15. KROLL, N. and JAIN, R.K. Solution of two dimensional euler equations – experience with a finite volume code. Technical Report DFVLR-FB 87-41, DLR, October 1987.
16. RAO, G.V.R. Exhaust nozzle contour for optimum thrust. *J Jet Propulsion*, June 1958, **28**, (6), :377:382.
17. TAYLOR, N.V. and HEMPSELL, C.M. Throat flow modelling of expansion deflection nozzles. JBIS, 57(7/8):242-250, 2004.
18. TAYLOR, N.V. and HEMPSELL, C.M. CFD and analytical methods for advanced nozzle calculations, presented as paper IAF-01-S.2.07 at the 2001 IAF conference, Toulouse.
19. TANNER, M. Steady base flows. *Progress in Aerospace Sciences,* 21:18-157, 1984.
20. TANNER, M. Two different theoretical approaches to the base pressure problem in two-dimensional flow. Technical Report DFVLF, Germany, May 1978.
21. MUELLER, T.J. Determination of the turbulent base pressure in supersonic axisymmetric flow. *J Spacecraft*, January 1968, **5**, (1), pp 101-107.
22. KORST, H.H. A theory for base pressures in transonic and supersonic flow. *J Applied Mechanics*, December 1956, **23**, (4), pp 593-599.
23. CHAPMAN, D.R. An analysis of base pressure at supersonic velocities and comparison wih experiments. Technical Report 1051, NACA, 1951.
24. TANNER, M. Base pressure in supersonic flow; further thoughts on a theory. *AIAA J*, February 1992, **30**, (2), pp 565-566.
25. CUFFEL, R.F., BACK, L.H. and MASSIER, P.F. Transonic flowfield in a supersonic nozzle with small throat radius of curvature. *AIAA J*, July 1969, **7**, (7), pp 1364-1366.